Desalination and Water Treatment
www.deswater.com

doi: 10.5004/dwt.2017.21545

99 (2017) 27–33
December

A computational tool for the estimation of the optimum gradient magnetic field for the magnetic driving of the spherical particles in the process of cleaning water

Evangelos G. Karvelas[a,*], Nikolaos K. Lampropoulos[b], Theodoros E. Karakasidis[a], Ioannis E. Sarris[b]

[a]*Laboratory of Hydromechanics and Environmental Engineering, Department of Civil Engineering, University of Thessaly, Volos 38334, Greece, Tel. +30-210-538-5382; Fax: +30-210-538-5306; email: karvelas@civ.uth.gr (E.G. Karvelas)*
[b]*Department of Energy Technology, Technological & Educational Institute of Athens, 12210, Greece*

Received 20 December 2016; Accepted 29 May 2017

ABSTRACT

The use of magnetic nanoparticles for cleaning potable water from heavy metals is a novel technique. Suitable magnetic fields are imposed in order to separate magnetic nanoparticles from the water main stream. A numerical methodology that combines computational fluid dynamics and evolution strategy techniques for the optimum magnetic navigation of particles in water is presented here. The method is based on an iterative algorithm that aims to minimize the deviation of particles from a desired trajectory by continuously adjusting a gradient magnetic field in an appropriate way. For the evaluation of the performance of this computational method, several series of simulations are performed with different number of adjustments of the magnetic field gradient. Using the above-mentioned method, it is found that the increase of the number of adjustments of the magnetic field gradient results in the decrease of the particles' deviation from the desired trajectory. Finally, the percentage of particles that are following the desired trajectory increases as the concentration of the simulated particles increases.

Keywords: Magnetic driving; Spherical particles; CFD; Heavy metals; CMA evolution strategy; DEM

1. Introduction

Increasing pollution of groundwater and surface water from a wide variety of industrial, municipal and agricultural sources has provoked serious water quality problems in these water resources, resulting in a reduction of the supply of freshwater for human use [1]. Although the nature of pollution problems may vary, some typical reasons are due to inadequate sanitation, algal blooms, detergents, fertilizers, pesticides, chemicals, potentially toxic metals, salinity caused by widespread and inefficient irrigation, and high sediment loads resulting from upstream soil erosion [2]. Thus, water scarcity is being recognized as a present and future threat to human activity and as a consequence, water purification technologies are gaining major worldwide attention [3]. In this perspective, biochemical or biotechnological nanotechnology has been identified as a promising technology that could play important roles in resolving potable water problems, involving water purification and quality [4].

Treatment and remediation of water contaminated with hazardous substances may be one of the most significant environmental applications of nanoparticles technology. Among the nanosized materials, iron oxides play a major role in many areas of chemistry, physics and materials science. In particular, magnetic iron oxides (Fe_3O_4) and magnetite (Υ-Fe_3O_4) have been investigated intensively for environmental applications [5–8]. Facilitated separation from water by magnetic forces is the most attractive asset of magnetic

* Corresponding author.

Presented at the conference on Efficient and Sustainable Water Systems Management toward Worth Living Development, 2nd EWaS 2016, Chania, Greece, June 1–4, 2016.

1944-3994/1944-3986

nanoparticles. Moreover, low toxicity, price and high surface to volume ratio, which is associated to their ability to adsorb pollutants on their surface, are additional advantages of iron oxide nanoparticles [9–14]. These surface chemicals can present enhanced capacity for heavy metals uptake in water treatment procedures. Using paramagnetic core materials, nanoparticles magnetic response is maximized, since they form chains under the influence of constant magnetic fields. The size of aggregates and their navigation into the desired areas is very important and depends on various parameters [15,16].

In this study, a computational platform for the calculation of the optimum gradient magnetic field for the separation of magnetic nanoparticles from clean water is presented in a purification process. Consequently, the computational platform is used in order to optimize the efficiency in the navigation process. In Section 2, the numerical methodology for the water flow and particles' motion and the simulation details are described. In Section 3, results and discussions are presented for the influence of different number of magnetic field gradient adjustments and number of particles inserted into the flow. Finally, conclusions are presented in Section 4.

2. Numerical model

2.1. Governing equations

The water flows in the channels of the Y-shaped (2D) microfluidic device with a rectangular cross-section and is expected to be laminar and steady-state. The incompressible Navier–Stokes equations are solved for the Eulerian frame together with a model for the discrete motion of particles in a Lagrangian frame. The laminar governing equations of the fluid phase are given as following:

$$\nabla \cdot u = 0 \tag{1}$$

$$\rho\left(\frac{\partial u}{\partial t} + u \cdot \nabla u\right) = -\nabla p + \mu \nabla^2 u \tag{2}$$

where t is the time, u and p are the fluid velocity and pressure, respectively, and ρ and μ are its density and viscosity, respectively.

The equations of every particle single motion in the discrete phase are based on the Newton law and may read as follows:

$$m_i \frac{\partial u_i}{\partial t} = \boldsymbol{F}_{\mathrm{mag},i} + \boldsymbol{F}_{\mathrm{nc},i} + \boldsymbol{F}_{\mathrm{tc},i} + \boldsymbol{F}_{\mathrm{drag},i} + \boldsymbol{F}_{\mathrm{grav},i} \tag{3}$$

$$I_i \frac{\partial \omega_i}{\partial t} = \boldsymbol{M}_{\mathrm{drag},i} + \boldsymbol{M}_{\mathrm{con},i} + \boldsymbol{T}_{\mathrm{mag},i} \tag{4}$$

where the index i stands for the ith-particle with diameter d_p, $\boldsymbol{u}_i$ and $\boldsymbol{\omega}_i$ are its transversal and rotational velocities, respectively, and m_i is its mass. The mass moment of inertia matrix is I_i, the terms $\frac{\partial \boldsymbol{u}_i}{\partial t}$ and $\frac{\partial \boldsymbol{\omega}_i}{\partial t}$ correspond to the linear and angular accelerations, respectively. $\boldsymbol{F}_{\mathrm{mag},i}$ is the total magnetic force, and $\boldsymbol{F}_{\mathrm{nc},i}$ and $\boldsymbol{F}_{\mathrm{tc},i}$ are the normal and tangential contact forces, respectively. $\boldsymbol{F}_{\mathrm{drag},i}$ stands for the hydrodynamic drag force, $\boldsymbol{F}_{\mathrm{grav},i}$ is the total force due to buoyancy, $\boldsymbol{M}_{\mathrm{drag},i}$ and $\boldsymbol{M}_{\mathrm{con},i}$ are the drag and contact moments, respectively, and finally, $\boldsymbol{T}_{\mathrm{mag},i}$ is the torque due to the magnetic field at the position of particle i.

The OpenFoam platform was used for the calculation of the flow field and the uncoupled equations of particles' motion [17]. Details of the numerical models, forces and moments terms used on particles are given in [18,19].

For the evaluation of the potential of the computational model a Y-shaped geometry is studied here, as depicted in Fig. 1(a). The angle between the two outlet branches is kept fixed to 60°and the overall length of the simulated channel is 36 mm. The computational grid for the geometry studied here is composed by 12,000 triangles with sufficient resolution of boundary layers is shown in Fig. 1(b). For the steady-state motion of the water, a constant pressure drop between the inlet and the outlets is imposed. As a result of the constant pressure drop, water flow with mean inlet velocity 12.2 mm/s is developed. In addition, no slip boundary conditions are applied at the solid walls.

The following numerical solution procedure is followed. In a first place, the calculation of the flow field is achieved by using the pressure implicit with splitting of operator method. When the flow and pressure fields are determined, the discrete motion of particles is evaluated by solving Eqs. (3) and (4) along the trajectory of each particle according to the discrete element method (DEM) [19]. The covariance matrix adaptation (CMA) evolution strategy algorithm [20] is used frequently to modify the magnitude of the gradient magnetic field. The equations are solved in time with the Euler time marching method. Representative duration of the numerical simulations from the present numerical models for 8 and 18 variations of the gradient magnetic field is 156 and 408 h of CPU time, respectively.

2.2. CMA algorithm to determine the most appropriate magnetic gradients

The CMA evolution strategy algorithm [20] is used to navigate the particles into a desired path through successive

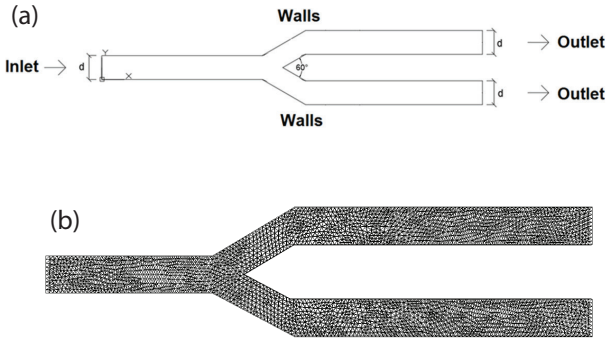

Fig. 1. (a) Channel geometry and boundary conditions. The width of the outlets is the same as the width of the inlet, and equal to d = 2.25 mm. (b) Schematic representation of the grid distribution for the channel with the same width between inlet and outlets.

variations of the magnetic gradient magnitude and sign. The CMA algorithm conducts an iterative principal components analysis of successful search steps, while retaining all principal axes. In addition, two paths of the time evolution of the mean distribution are recorded, called search or evolution paths, respectively. These paths include significant information about the correlation between consecutive steps.

In particular a gradient magnetic field is selected by sampling a multi-variate normal distribution. The basic equation for sampling the gradient magnetic fields, for generation number $g = 0,1,2, \ldots$ is $\boldsymbol{x}_k^{(g+1)} \sim N(m^{(g)}, (\sigma^{(g)})^2 C^{(g)})$ for $k = 1, \ldots, \lambda$, where $\sim$ indicates the same distribution on the left and the right side, $\boldsymbol{x}_k^{(g+1)} \in \mathbb{R}^n$, kth offspring (search point) form generation $g + 1$, $\boldsymbol{m}^{(g)} \in \mathbb{R}^n$, mean value of the search distribution at generation g, $\sigma^{(g)} \in \mathbb{R}_+$, overall standard deviation, step size, at generation g, $\boldsymbol{C}^{(g)} \in \mathbb{R}^{n \times n}$, covariance matrix at generation g, and $\lambda \geq 2$, population size, sample size, number of offspring.

The method intends to minimize the particles' position deviation from a desired trajectory. The trajectory in all present simulations is predefined in the computational platform by a 10 degree polynomial. In this way, the gradient magnetic field is temporarily adjusted as described in the following section so as the particles' distances from the desired trajectory is minimized.

2.3. Optimum driving process

Initially, the steady-state water flow in the microchannel, Fig. 1(a), is achieved by suitably solving Eqs. (1) and (2). Water loaded with particles enters the channel from the left and splits into the two outlet branches at the right side of the domain.

Once the flow and the pressure fields are found, the discrete phase simulation starts with combination of the DEM and the CMA methods. The CMA provides DEM with random values of a gradient magnetic field in the beginning. The DEM method evolves all particles' positions for some time and the distance between the particles and the desired trajectory is checked. The CMA works in order to minimize this distance and then provides a new value of the gradient magnetic field, as is shown in Fig. 2. In this way, the appropriate values of the gradient magnetic field are found for the particles' navigation into the targeted areas, as is depicted in Fig. 3, for the case of 8 adjustments. If all particles are in the desired trajectory, the simulation ends.

Different quantities of particles with hydrodynamic diameter equal to 1 μm are simulated. The study covers the range from 10 to 1,000 particles in order to examine the influence of the particle's number in the navigation. Initially, all particles enter the channel from random positions of the inlet. The simulations are performed under a uniform transverse magnetic field $B_0 = 1T$ and the performance of the CMA method is studied for gradient magnetic field adjustments in the range of ±500 mT/m.

3. Results

Series of simulations are performed with different numbers of gradient magnetic field adjustments in order to evaluate the effect of the number of adjustments in the navigation for magnetic particles. Four scenarios of different number of adjustments of the magnetic field gradient are selected and the particles' centre distance from the desired trajectory is

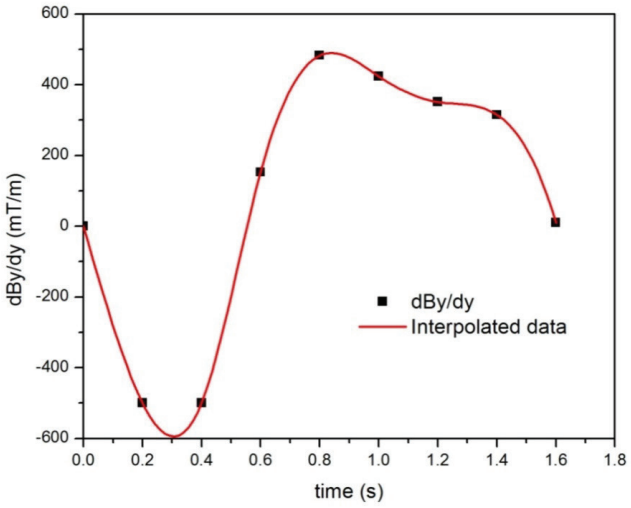

Fig. 3. Predicted magnitudes of CMA of the gradient magnetic field (case of 8 magnetic gradient adjustments) for the navigation of particles in Fig. 2.

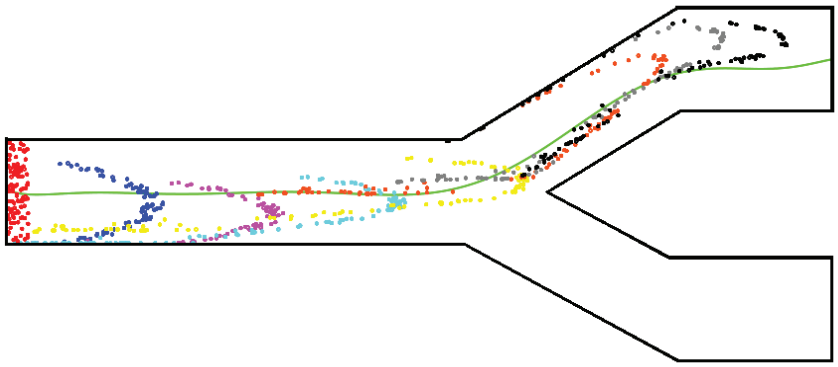

Time step	Color
Initial	Red
0.2 s	Blue
0.4 s	Pink
0.6 s	Cyan
0.8 s	Yellow
1 s	Orange
1.2 s	Grey
1.4 s	Black

Fig. 2. Desired trajectory (Green) and positions of particles in each time step obtained by application of gradients presented in Fig. 3.

measured just at the moment before particles exit the domain and an average over all particles is performed. This distance is representative of how close the particles are to the desired trajectory. As we can see in Fig. 4, the increase of the number of the magnetic gradient adjustments, results in better driving of the particles close to the desired trajectory. The observed decrease of the particles' distance in relation to the desired trajectory seems to present a non-linear behaviour as a function of the number of adjustments of the magnetic field gradient.

On the same figure we can see that the number of particles influences the deviation of the particles from the desired trajectory. As we can see for a few particles, that is, only 10 particles, the increase of frequency of the magnetic gradient adjustments plays almost insignificant role. This is coherent with previous findings [18] and it is connected to the magnetic moment of particles. As the number of particles increases, aggregations under constant magnetic fields are easier to form and thus particles can be navigated easier by gradient magnetic fields. As a consequence, when we have only 10 particles, it is more difficult to move them along the desired trajectory than in the case of 1,000 particles. Moreover, we can see in Fig. 4 that the CMA algorithm can navigate almost with the same deviation from the trajectory all particles when their number is above 200.

The increasing number of adjustments of the gradient magnetic field during the flow of the particles from the inlet to the outlet, not only decreases the particles' distance from the desired trajectory but also it seems to affect the distribution of particles in the channel around the desired trajectory. As we can see in representative results in Fig. 5(a) with 8 adjustments we have the particles distributed around the desired trajectory with larger distances from it compared with the case of 18 adjustments (Fig. 5(b)). For 8 adjustments (Fig. 5(a)), single particles and aggregations can be found almost everywhere near the outlet of the channel. In the case of 18 adjustments, however, a single chain that consists of almost all particles and only a few single particles are found close to the selected trajectory near the outlet of the channel (Fig. 5(b)). Thus, the present navigation algorithm appears to be very efficient as the number of adjustments of the magnetic field gradient increases.

A more quantitative result is given in Fig. 6 where the percentage of particles that can be found within a distance $\pm d_i$ around the selected location of the desired trajectory is plotted against the frequency of magnetic gradient adjustments. An almost linear increase of the particles number is found with the increase of magnetic field gradient adjustments (above 8). Moreover, as particles number increases, more particles can be found near the desired trajectory, due to the increasing concentration of particles inside the channels. As a consequence, the percentage of particles that is located within a distance $\pm d_i$ around the desired trajectory is expected to be large enough, since in a real life scale device billions of particles will be used.

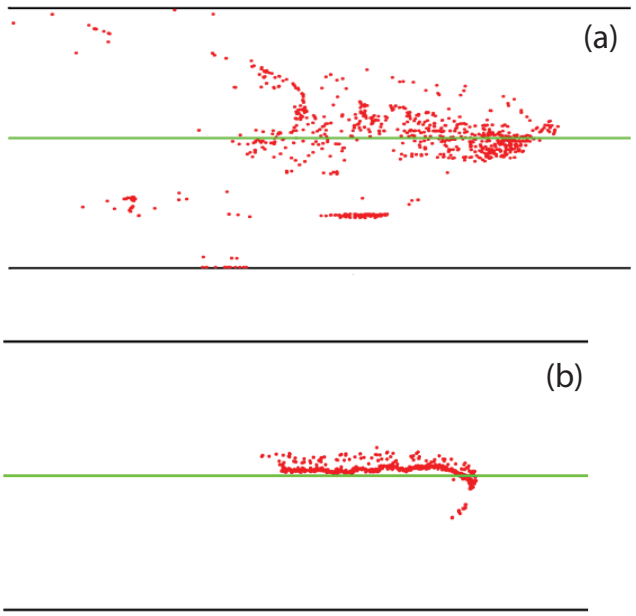

Fig. 5. Particles distribution snapshots near outlet for (a) 8 adjustments of the magnetic gradient and (b) 18 adjustments of the magnetic gradient. Outer lines (in black) represent boundaries (walls), while the middle line (in green) the desired trajectory.

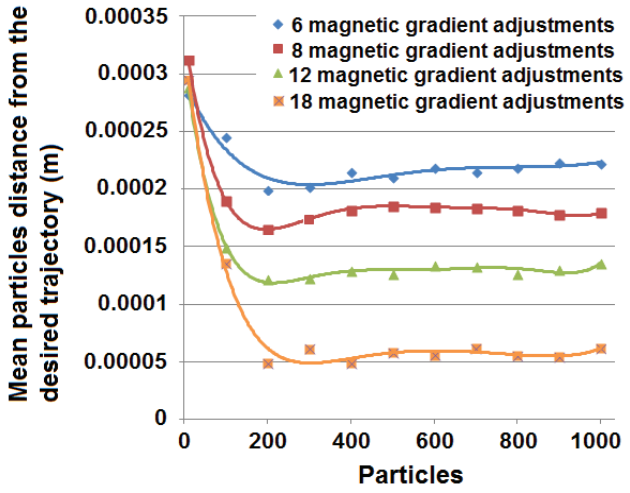

Fig. 4. Mean particles distance from the desired trajectory for different number of particles under the influence of different number of magnetic gradient adjustments.

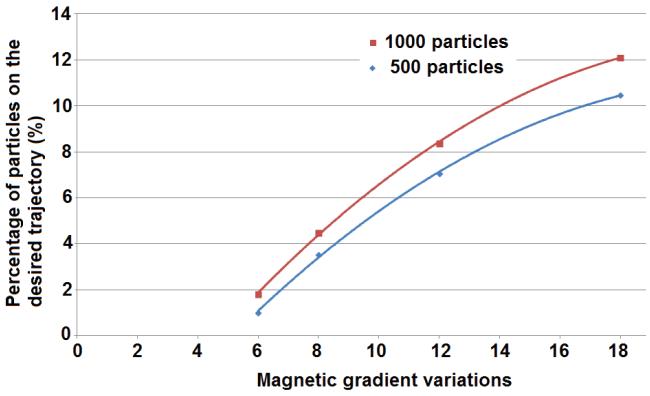

Fig. 6. Percentage of particles on the desired trajectory against the frequency of the magnetic gradient adjustments.

As the number of magnetic gradient adjustments increases (as time passes) the driving of the particles becomes easier in the water, and the range of values of absolute magnitude of the magnetic field gradient is reduced as it can be seen in Fig. 7. We can clearly see therein that in the case of 6 adjustments a range of ±500 mT/m is applied while it is less than the half, that is, ±200 mT/m when 18 adjustments are used. The range of the magnetic field gradient that is used by the method, in the cases with 8 and 12 adjustments is ±450 and ±400 mT/m, respectively. Thus, by increasing the number of adjustments of the magnetic field gradient the corresponding applied range of gradients is significantly reduced (about 250% in the case of 18 adjustments in comparison with the case of 6 adjustments) and thus less resources are needed for the navigation.

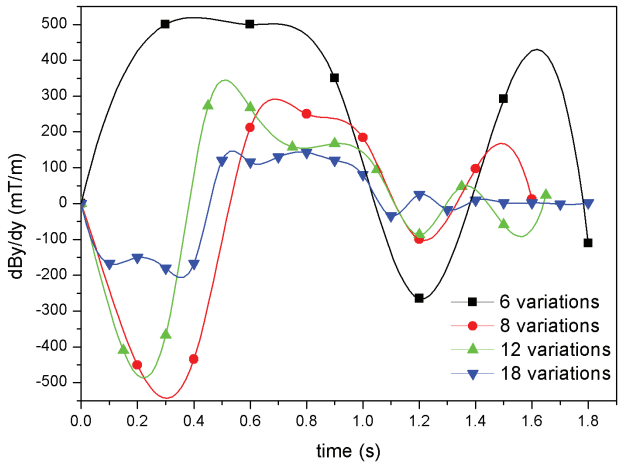

Fig. 7. Magnetic gradient magnitude distribution over time for different variations. Splines interpolation is selected for the continuous lines.

In the case of 6 adjustments, the magnetic gradients that are evaluated by the method are in the positive range for the first second of the simulation, in contrast with the cases of 8, 12 and 18 adjustments. This occurs due to the frequency of the imposed magnetic gradients and the positions of the particles, since these adjustments are applied in different times. In each scenario, the particles are located in different positions inside the channel for the first enforcement of the gradient magnetic field, as is depicted in Fig. 8. As it is observed in the scenario with 6 magnetic gradient adjustments, the particles have advanced nearly up to the middle of the main branch's length when the first application of the magnetic field gradient nearly takes place. As a result, the magnetic gradient that is evaluated in order to drive the particles closer to the desired trajectory is the highest one among the cases that are simulated. As we can see in Figs. 8(b) and (c), the particles, in the rest of the scenarios, are located closer to the inlet and are less spread thus are easier to manipulate. In the cases with 8 adjustments or more, the frequency of the adjustments seems to be enough for a completely different profile of the gradient magnetic adjustments, as is depicted in Fig. 7. The increase of the adjustments leads to lower ranges of the gradient magnetic field since after each adjustment the particles are closer

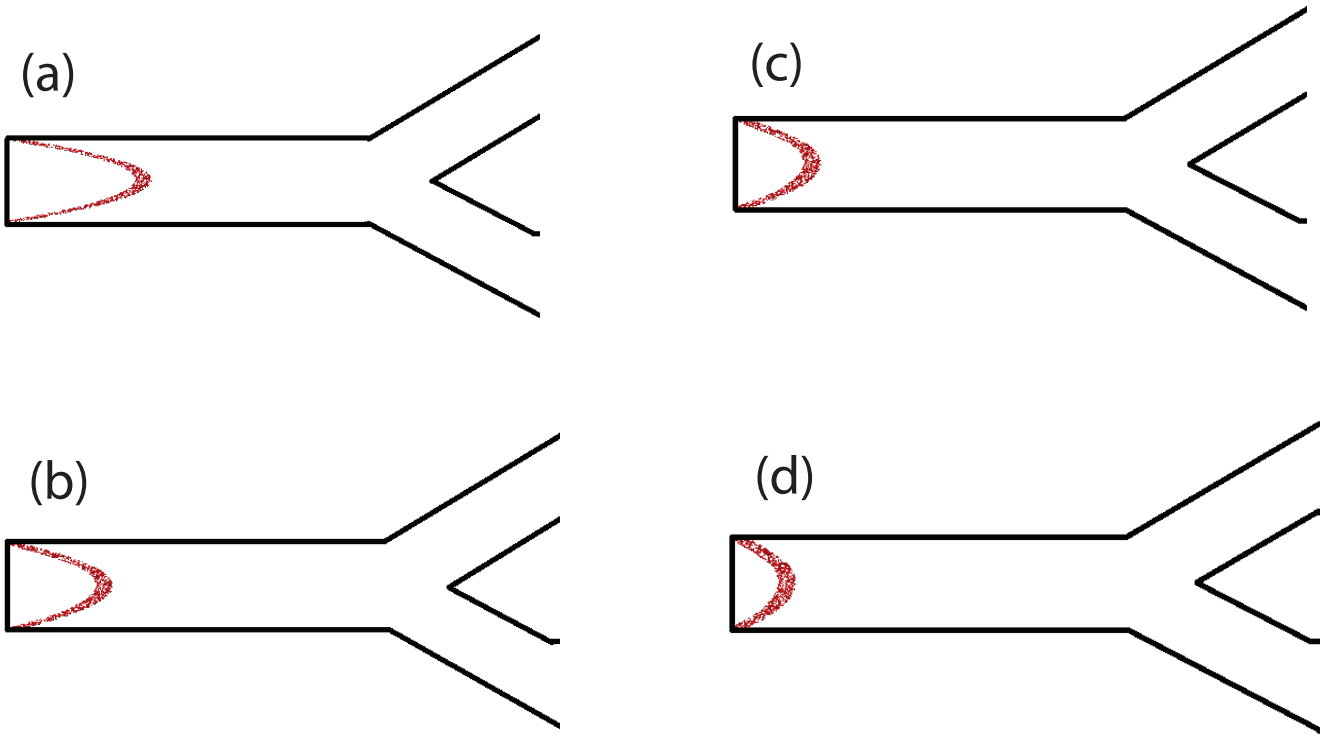

Fig. 8. Snapshot of the positions of particles just before the enforcement of the gradient magnetic field for different scenarios; (a) 6 magnetic gradient adjustments, 0.3 s (b) 8 magnetic gradient adjustments, 0.2 s (c) 12 magnetic gradient adjustments, 0.15 s and (d) 18 magnetic gradient variations, 0.1 s (only the entrance of the particles is presented).

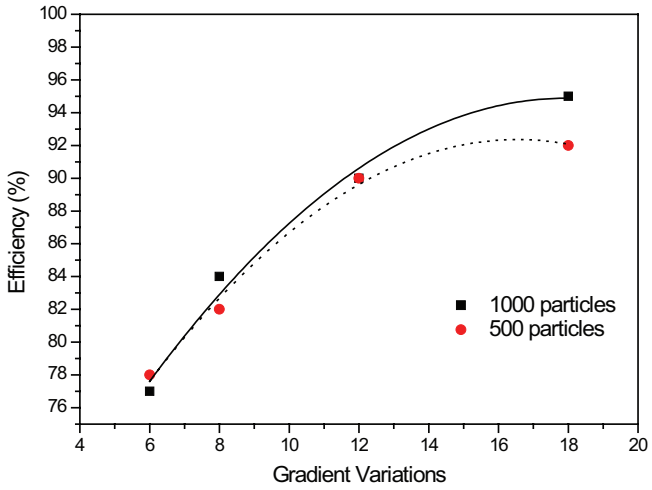

Fig. 9. Efficiency of CMA algorithm for the navigation of particles in the outlet of the channel for different magnetic gradient adjustments and number of particles.

to the desired trajectory. The frequency of the magnetic gradient adjustments is the most significant parameter for an increased efficiency of the driving process as is depicted in Fig. 9.

As the magnetic gradient adjustments are increased, the efficiency of the CMA algorithm navigation of particles in the right outlet channel is getting higher as is depicted in Fig. 9. For 6 magnetic gradient adjustments only 75% of the simulated particles are following the desired trajectory, while for 18 magnetic gradient adjustments this efficiency can reach over 90%. Increase in the navigation efficiency is also recorded as the number of particles increases as commented also in the results of Fig. 6. It is also observed that for each number of simulated particles a plateau on the efficiency of the navigation is reached as the number of magnetic gradient adjustments increases. This is connected with the aggregation process, where slow single particles are trapped close to the walls, cannot attract other particles in order to make aggregations and cannot follow the vast majority of particles in the navigation process.

4. Conclusions

In this work, a computational method for the estimation of the optimum values of the magnetic field gradient for the navigation of a certain amount of magnetic nanoparticles in a water flow along a desired trajectory is presented. Different simulations were conducted in order to evaluate the performance of the proposed methods as a function of several parameters. Parameters include the number of adjustments of the magnetic field gradient, the magnitude of the employed magnetic field gradient and the number of nanoparticles inserted into the flow.

The computational method that is presented can achieve efficiency above 90% in magnetic navigation of a certain amount of particles through a desired path. The increase of the magnetic field gradient adjustments results in a decrease of the particles' distance from the desired trajectory. In addition, an increased number of magnetic field gradient adjustments results in a reduced magnitude of the magnetic field gradient that has to be applied in order to drive the particles. The computational method can be used with optimum efficiency in terms of driving of the particles in small tubes and has the potential to estimate the appropriate deviation of the magnetic field during the particles' navigation into micromixers.

The developed method can be employed for the particles' removal from potable water. Moreover, it can optimize the particles' driving and evaluates the optimum range values of the gradient magnetic field. As a result, the particles do not remain stuck in the walls of the channels. This leads to the optimization of the cleaning water efficiency, as all the particles can be re-used. Using the above mentioned method, the sizing of water treatment systems can be easily calculated in order to minimize the operating cost. Finally, the efficient operation of the method contributes to minimizing of health problems that occurred due to the existence of heavy metals on the potable water.

References

[1] J.A. Foley, R. DeFries, G.P. Anser, C. Barford, G. Bonan, S.R. Carpenter, F.S. Chapin, M.T. Coe, G.C. Daily, H.K. Gibbs, J.H. Helkowski, T. Holloway, E.A. Howard, C.J. Kucharik, C. Monfreda, J. Patz, I. Prentice, N. Ramankutty, P.K. Snyder, Global consequences of land use, Science, 309 (2005) 570–574.
[2] I.R. Falconer, A.R. Humpage, Health risk assessment of cyanobacterial (blue-green algal) toxins in drinking water, J. Environ. Res. Public Health, 2 (2005) 43–50.
[3] J. Theron, J.A. Walker, T.E. Cloete, Nanotechnology and water treatment; applications and emerging opportunities, Crit. Rev. Microbiol., 34 (2008) 43–69.
[4] J.Y. Bottero, J. Rose, M.R. Wiesner, Nanotechnologies: tools for sustainability in a new wave of water treatment processes, Integr. Environ. Assess. Manage., 2 (2006) 391–395.
[5] F.B. Li, X.Z. Li, C.S. Liu, T.X. Liu, Effect of alumina on photocatalytic activity of iron oxides for bisphenol; a degradation, J. Hazard Mater., 149 (2007) 199–207.
[6] A.L. Daniel-da-Silva, R. Lóio, J.A. Lopes-da-Silva, T. Trindade, B.J. Goodfellow, A.M. Gil, Effects of magnetite nanoparticles in the thermorheological properties of carrageenan hydrogels, J. Colloid Interface Sci., 324 (2008) 205–211.
[7] Y.F. Shen, J. Tang, Z.H. Nie, Y.D. Wang, Y. Ren, L. Zuo, Preparation and application of magnetic Fe_3O_4 nanoparticles for wastewater purification, Sep. Purif. Technol., 68 (2009) 312–319.
[8] T.K. Indira, P.K. Lakshmi, Magnetic nanoparticles – a review, Int. J. Pharm. Sci. Nanotechnol., 3 (2010) 1035–1042.
[9] L. Guo, J. Li, L. Zhang, J. Li, Y. Li, C. Yu, J. Shi, M. Ruan, J. Feng, A facile route to synthesize magnetic particles within hollow mesoporous spheres and their performance as separable Hg^{2+} adsorbents, J. Mater. Chem., 18 (2008) 2733–2738.
[10] A.A. Atia, A.M. Donia, S.A. El-Enein, A.M. Yousif, Effect of chain length of aliphatic amines immobilized on a magnetic glycidyl methacrylate resin towards the uptake behavior of Hg(II) from aqueous solutions, Sep. Sci. Technol., 42 (2007) 403–420.
[11] Li et al., A novel technology for biosorption and recovery hexavalent chromium in wastewater by bio-functional magnetic beads, Bioresour. Technol., 99 (2008) 6271–6279.
[12] R.R. Sheha, A.A. El-Zahhar, Synthesis of some ferromagnetic composite resins and their metal removal characteristics in aqueous solutions, J. Hazard Mater., 150 (2008) 795–803.
[13] C. Huang, B. Hu, Silica-coated magnetic nanoparticles modified with γ-mercaptopropyltrimethoxysilane for fast and selective solid phase extraction of trace amounts of Cd, Cu, Hg, and Pb in environmental and biological samples prior to their determination by inductively coupled plasma mass spectrometry, Spectrochim. Acta, Part B, 63 (2008) 437–444.

[14] S. Shin, J. Jang, Thiol containing polymer encapsulated magnetic nanoparticles as reusable and efficiently separable adsorbent for heavy metal ions, Chem. Commun., 10 (2007) 4230–4232.
[15] N.K. Lampropoulos, E.G. Karvelas, I.E. Sarris, Computational study of particles interaction distance under the influence of steady magnetic field, Adv. Syst. Sci. Appl., 15 (2015) 227–236.
[16] E.G. Karvelas, N.K. Lampropoulos, T.E. Karasidis, I.E. Sarris, Computational study of the optimum gradient magnetic field for the navigation of the spherical particles in the process of cleaning the water from heavy metals, Procedia Eng., 162 (2016) 77–82.
[17] N.K. Lampropoulos, E.G. Karvelas, I.E. Sarris, Computational Modeling of an MRI Guided Drug Delivery System Based on Magnetic Nanoparticle Aggregations for the Navigation of Paramagnetic Nanocapsules, 11th World Congress on Computational Mechanics (WCCMXI) Barcelona, Spain, 2014.
[18] E.G. Karvelas, N.K. Lampropoulos, I.E. Sarris, A numerical model for aggregations formation and magnetic driving of spherical particles based on OpenFOAM, Comp. Methods Progr. Biomed., 142 (2017) 21–30.
[19] E. Tijskens, H. Ramon, J. Baerdemaeker, Discrete element modelling for process simulation in agriculture, J. Sound Vibr., 266 (2003) 493–514.
[20] N. Hansen, The CMA evolution strategy; a comparing review, Adv. Estim. Distrib. Algorithms, 192 (2006) 1769–1776.